UC Merced

UC Merced Previously Published Works

Title

Quantifying Varnish Removal Using Chemical Flushes

Permalink

https://escholarship.org/uc/item/4w47b8jc

Journal

Tribology transactions, 61(6)

ISSN

1040-2004

Authors

Johnson, Duval
Dominguez, Enrique
Montalvo, Elizabeth
et al.

Publication Date

2018-11-02

DOI

10.1080/10402004.2018.1468520

Peer reviewed

eScholarship.org Powered by the California Digital Library
University of California

Tribology Transactions 61 (2018) 1067

http://dx.doi.org/10.1080/10402004.2018.1468520

Quantifying Varnish Removal Using Chemical Flushes

Duval Johnson[1], Enrique Dominguez[2], Elizabeth Montalvo[2], Zhen Zhou[2], Ashlie Martini[1*]

1. Department of Mechanical Engineering, University of California Merced
2. Chevron Lubricants

* Corresponding Author: amartini@ucmerced.edu

ABSTRACT

Varnish deposits are a detrimental by-product of hydrocarbon oxidation that can ultimately result in component failure. Varnish is often removed by flushing a system with chemicals that soften the varnish, allowing suspension in the fluid, and removal by filter media. However, at this point it is difficult to evaluate the effectiveness of a chemical flushing compound because there is no standard technique for characterizing removal amounts and rates. Here, a test system is designed and built to address this issue. The system provides a means of characterizing the ability of a chemical compound to remove artificial varnish under carefully controlled conditions. Test metrics include mass loss and time-lapse, photographic data. The approach is demonstrated here by comparing two standard varnish removal chemicals and the findings establish the viability of the method as a standard test for characterizing varnish removal using chemical flushes.

INTRODUCTION

Varnish is formed as hydrocarbon base fluids degrade through oxidation. Oxidation is accelerated by exposure to increased temperatures, mechanical stresses, ultraviolet light, entrained air, electrostatic discharge and wear materials (metals) found in typical machines [1,2]. Varnish is formed as soluble primary oxidation products, such as acids, water and alcohols, follow condensation and polymerization reactions to form insoluble products [3]. These products are polar, causing varnish to adsorb on metal surfaces where further agglomeration thickens the varnish [4]. Varnish formation depends not only on the formation of polar compounds, but also upon the concentration of those compounds exceeding their solubility limit, which is temperature-dependent. Varnish typically has a gold-orange appearance that darkens as the thickness increases. However, varnish appearance can vary with factors such as base stock and additive package constituents, temperature, atmospheric content and surface material [5].

Varnish deposits are one of the most detrimental by-products of hydrocarbon oxidation [6,7]. Varnish fills the tight clearances between the valve and bore in hydraulic circuits causing erratic valve operation and in some cases fully seized valves [6]. Varnish contributes to decreased efficiency, increased wear and corrosion, impaired oil cooler performance and inadequate hydrodynamic lubrication. Journal bearings that experience varnish build up have increased shear rates, increased operational temperatures and, in extreme cases, bearing failure [8]. A sticking inlet guide vane valve of large frame gas turbines, such as those used in the power generation industry, can produce a fail to start, or shut-down event [9].

More efficient combustion processes have been achieved by increasing combustion temperatures [10]. This has strained the capabilities of materials and the lubricants that separate them. For temperatures greater than 100°C, each increase of 10°C doubles the rate of oxidation, which directly contributes to the inevitable formation of varnish and the eventual depletion of anti-oxidant compounds [11]. Internal combustion engines are well known for creating environments conducive to varnish formation where, in the ring pack of the piston, temperatures can exceed 250°C [12]. Air compressor temperatures can exceed 250°C, causing varnish formation which decreases the working clearances of rotor blades and robs efficiency [13]. The rapid compression of entrained air can produce temperatures in excess of 500°C and electrostatic discharge creates localized temperatures upwards of 10,000°C, causing thermal degradation of the fluid [14]. Temperatures such as these lead to accelerated rates of varnish formation and decrease the working life of the fluid.

The first steps in minimizing hydrocarbon oxidation are implemented at refineries where techniques are employed to remove undesirable components that are easily oxidized, such as unsaturated hydrocarbons, polar components and wax, from crude oil [3]. Synthetic oils are widely produced to combat thermal degradation by producing molecular chains that are fully saturated, uniform and predictable during formation. Further oxidative resistance is provided through the use of strong anti-oxidation compounds designed to work synergistically with other additives, thereby providing superior performance and degradation resistance [15].

Varnish mitigation methods are also implemented by removing primary oxidation products using electrostatic and adsorption methods. Electrostatic varnish mitigation takes advantage of the polar nature of varnish combined with dielectrophoresis to remove varnish and varnish pre-cursors. Adsorption typically uses filter media with pores small enough to retain oxidation by-products. While these methods are successful in removing degradation by-products, they require extended durations for optimal performance with no shut down time, and temperatures should be maintained in a range that allows varnish to remain in suspension and be removed by filtration. Furthermore, caution must be used when choosing filter media, which can inadvertently remove beneficial additive compounds from the fluid [16].

Varnish removal can also be performed using chemical flushing compounds. Flushing involves circulation of fluid through the lubrication system or a component to remove varnish or other contaminants. ASTM D6439 provides guidelines for flushing turbine lubrication systems [17]. While the electrostatic and adsorption methods are *re-active* to the formation of varnish, the chemical flush is *pro-active* in removing varnish. Chemical flushing compounds soften varnish, allowing it be suspended in the fluid and removed by filter media. This process can be very fast, depending on the chemicals used, and allows the system to remain fully functional while the cleaning process occurs. Moreover, the removal of additive package compounds by filtration is not a concern since a full oil change will occur when the process is complete, allowing very fine filter media to be used.

One issue with varnish mitigation and removal has been a lack of standard methods to characterize removal amounts and rates. This is in sharp contrast to the many standards that are available to characterize an oil's resistance to oxidation, the precursor to varnish formation, e.g. ASTM D974 or D664 [18,19], ASTM D2272 [20], ASTM D445 [21], ASTM D92 [22]. Such standards provide consistent methods for testing lubricating oils before and during use, but it is equally important to quantify and standardize varnish removal. Standardized testing for varnish removal by chemical flushing

could ultimately enable direct comparison of the effectiveness of chemical compounds as well as guidance for selecting a compound for a given application.

To address this, a test has been designed to quantify varnish removal using chemical cleaners. The test system has been designed to allow control of flow rates and temperatures across a flat steel sample containing artificial varnish. The artificial varnish is produced using common oxidative mechanisms and is characterized to ensure the material accurately simulates varnish produced within a gas turbine engine. The varnish is then subjected to chemical flushes at controlled flow rates and temperatures. Testing metrics include mass loss and time-lapse video data, where the latter is analyzed quantitatively to determine performance parameters, including the maximum rate of varnish removal. The approach is demonstrated by comparing two typical chemical flushing compounds. Results show that the new test approach provides a consistent and reliable way to evaluate chemical flush effectiveness.

METHODS

The artificial varnish used for the test system is formed by reproducing oxidation mechanisms, similar to those expected to occur in gas turbine engines, in the lab. The artificial varnish is prepared by, first, aging a mineral base oil sample per common lube oil aging tests, such as ASTM D7873 [23]. Then, the aged oil is filtered and sludge samples are collected. Next, 100 mg of the sludge is applied to a steel coupon. The varnish coupons are placed in the oven for 3 hours at 135 C. After baking, the varnish outside of a prescribed area in the center of the coupon is removed. A representative coupon with varnish is shown in Figure 1a. The result is characterized using Fourier-transform infrared spectroscopy (FTIR), shown in Figure 1b. The analysis reveals that the artificial varnish exhibits peaks associated with gas turbine oil degradation. The FTIR data also provides estimates of the composition weight percent and the artificial varnish is found to contain 70% C, 9% H, ~20% O and less than 1% N, Fe and Cu. These results indicate that the artificial varnish is a reasonable approximation of varnish that might occur during component use. Each coupon is weighed prior to testing.

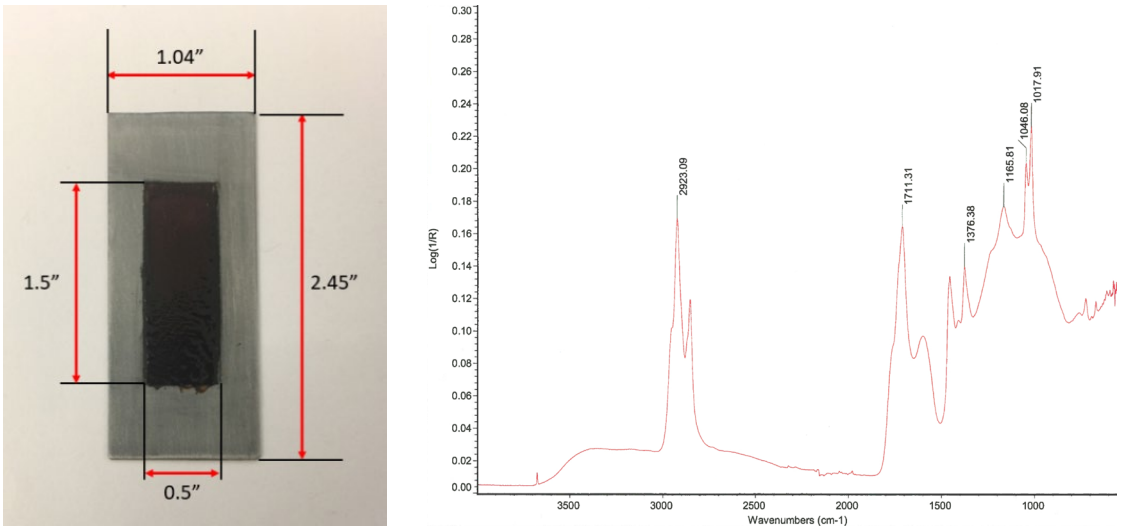

(a) (b)

Figure 1: (a) Photo of a representative steel coupon with varnish before testing, showing the dimensions of the coupon and varnish. (b) FTIR analysis of artificial varnish created in the lab that exhibits peaks consistent with what is expected for varnish produced by gas turbine oil degradation.

The test system is comprised of nine main components, as shown in Figure 2. Test system flux is provided by an electric motor, which has a V/F inverter, coupled to a vane pump. An adjustable pressure relief valve is set to bleed any pressure over 150psi while a variable area flow meter tracks total flow through the system. A 3-way ball valve is used to divert flow from the main line to a by-pass line metered by a very accurate positive displacement flow meter. The desired flow is then directed through the test cell where the coupon is housed. The fluid, with any removed varnish particles, is filtered and then returned to the reservoir passing over the heating coils.

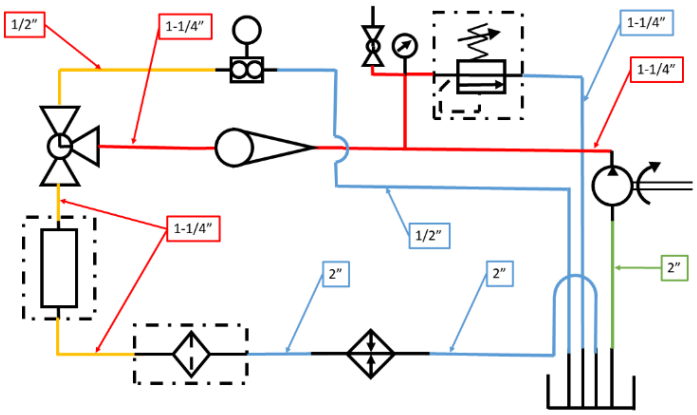

Figure 2: Test system schematic showing the nine main components including: pump, pressure relief valve, variable area flow meter, 3-way ball valve, test cell, filter, heater, positive displacement flow meter and reservoir.

The test system can provide flow rates varying between 0.1<Q(GPM)<48 through the test cell, and the temperature capabilities range from 40<T(°C)<120. Depending on the viscosity of the fluid (tests

reported here conducted with an ISO-46 fluid) being tested, the Reynolds numbers that can be generated within the test cell range from 10<Re<40,000.

The heart of the test system is the test cell. Figure 3 shows a schematic and photo of the test cell. The design ensures that the entire surface of the varnish is exposed to the flow of oil. The placement of the coupon in the test cell is such that the top of the coupon, where the varnish resides, is flush with the bottom of the incoming pipe wall. This provides a continuous no slip condition from the pipe wall to the coupon, thereby exposing only the varnish into the flow of oil. This simulates many environments where varnish is formed on the no slip boundary conditions of machinery. The lid of the test cell is made of vapor polished polycarbonate allowing a camera to be positioned above the coupon for recording.

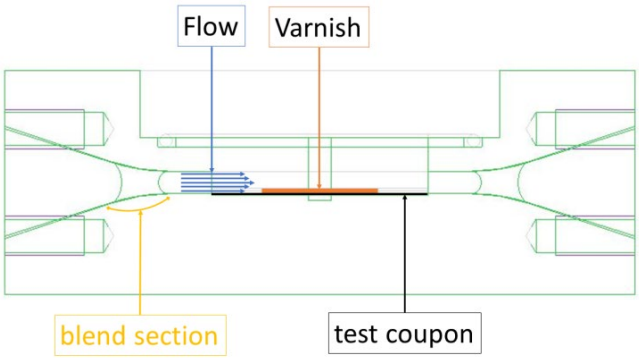

(a)

(b)

Figure 3: (a) Wireframe CAD model of test cell showing location of coupon and varnish. (b) Photo of the test cell without the polycarbonate lid. The varnish coupon prior to testing can be seen in the center of the cell. Dimensions on both figures correspond to the scale bar shown in the lower right corner of (b).

Each test is preceded by flushing the system with the base stock to remove any remaining fluid from the previous test. First, the system is drained and air is injected into the system for 5 minutes to remove previous test fluid. Then, the system is flushed with 5 gallons of base fluid for 20 minutes, for a total of 90 gallons of flow. Finally, a new test fluid is added to the system and circulated through both the main and by-pass lines.

The system is initially run without the coupon until the temperature reaches steady state. Then, the flow is stopped temporarily and a prepared coupon is inserted into the test cell. The camera lighting is turned on and photographic recording begins. The system is turned back on and the desired duration of testing is performed. During the test, images are captured using a 12.0 MP resolution camera set to take a photograph every 10 seconds. The placement of the camera is fixed so that the position of the varnish is the same for all tests. Upon completion of the test, the coupon is removed from the test cell and dried in heptane to remove any oil from the sample prior to weighing. An initial post-test mass recording is done and 24 hours later another is performed to ensure no further change occurred due to evaporating heptane. The difference between the pre-test and post-test mass is identified as mass loss, one of the metrics used to characterize varnish removal.

Here, the test system is demonstrated here with two fluids, Fluid A and Fluid B, both of which are known to have varnish removal capabilities. Both fluids are commercial cleaners blended at the same weight percentage with a 46 cSt (at 40°C) base oil. The chemical components of these commercial cleaners are unknown. However, the flash point of the commercial cleaner in Fluid A (<100°C) was much lower than that of the commercial cleaner in Fluid B (>200°C), which indicates higher light solvent content in Fluid A.

All tests are conducted at a temperature of 90°C, a flow rate of 4.5GPM and a duration of 120 minutes. With a flow rate of 4.5GPM, an average velocity of 10.12 ft/s (3.08 m/s) is created within the test cell. The viscosities of the two fluids tested are 17.27 and 12.82 centi-Stokes (cSt) at 90°C, which correspond to Reynolds numbers in the high laminar flow regime (Re_A=1,442 and Re_B=1,944). These conditions are selected to approximate lubrication conditions in a gas turbine engine, as well as to optimize the test in terms of sufficient varnish removal with a minimum test time. Two tests are run for each fluid under these conditions.

RESULTS

The mass loss results for the two tests performed on each fluid are shown in Figure 4. There is a significant difference between the total mass removed by Fluid A and Fluid B during the 120 minute test. On average, Fluid A removed 95.9% of the varnish while Fluid B removed 46.9%. The error in the two measurements is 1% for Fluid A and 34% for Fluid B. However, despite the relatively large error for Fluid B, the difference between the two fluids is statistically significant, i.e. the minimum removed by Fluid A (95.4%) is much greater than the maximum removed by Fluid B (56.7%). Although the composition of these fluids is not known, the properties of Fluid A indicate it has a higher light solvent content, which may explain why it is able to remove more varnish.

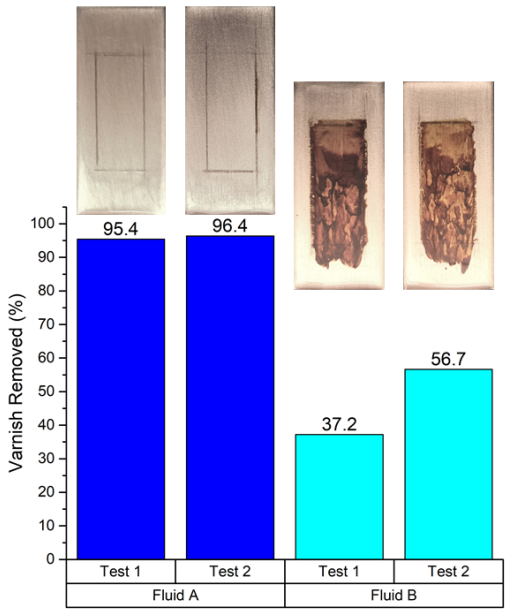

Figure 4: Percent varnish mass removed during the 120 minute tests on Fluid A and B. Insets show photos of the coupons after each of the tests.

The mass loss results are informative and clearly illustrate a difference between the two fluids. However, the images taken during testing can be used to provide more information about varnish removal. An algorithm is developed to analyze the images of the varnish coupons taken during the test using the CMKY color scale. An illustration of this algorithm is shown in Figure 5. First, an image of the test cell before the test is taken and the image is cropped to include just the coupon. Then, a region with no varnish is identified and the average K value is calculated from that region to use as the no-varnish reference (K_{min}). This is repeated for a region with only varnish (K_{max}). Then, during the test, the average K value of the varnish region is obtained. After the test, the K values at each time are normalized using the references K_{min} (no varnish) and K_{max} (maximum amount of varnish). This step ensures that the algorithm can be applied for any varnish or fluid, i.e. having any initial appearance or color.

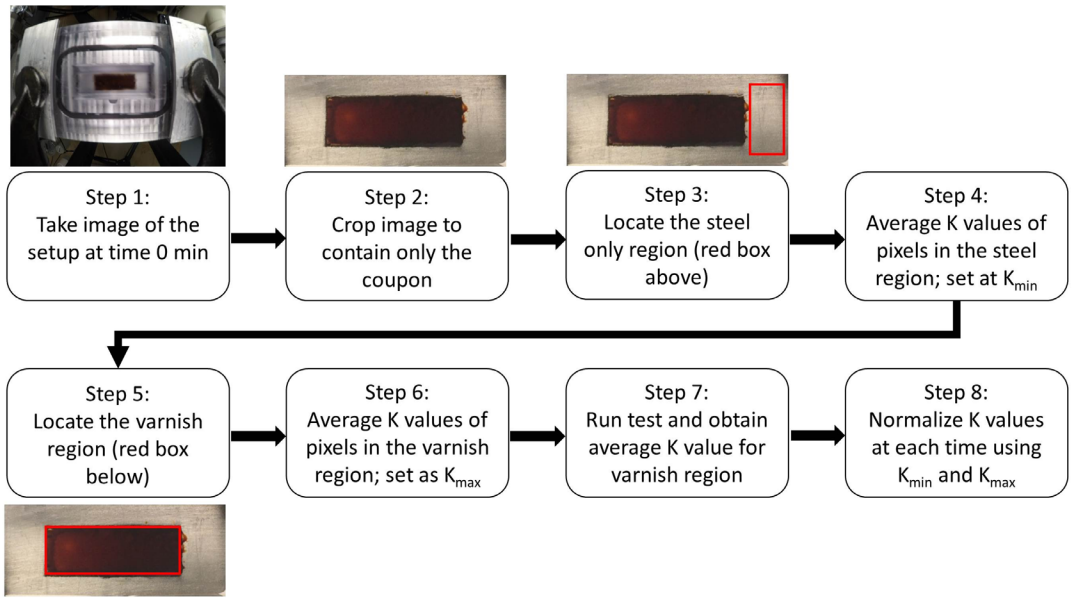

Figure 5: Algorithm used to quantify varnish removal including: 1-original image, 2-cropped image, 3-location of steel reference site, 4-averaging steel values, 5-locating varnish region, 6-averaging varnish K values, 7-collect data during test and 8-normalize data to generate a plot of the amount of varnish as a function of time.

The results of this analysis for the two fluids are shown in the top panels of Figure 6. The normalized K value necessarily starts at 1 and then decreases as the varnish is removed as the test proceeds. It can be observed that the rate of change of the K factor with time is faster for Fluid A, indicating that this fluid removes varnish more quickly. Fluid A also reaches steady state varnish removal sooner than Fluid B. These observations can be quantified by taking the derivative of the K factor vs. time data, as shown in the lower panels of Figure 6. First, the time of the maximum varnish removal rate can be identified from the maximum negative value of the derivative. Second, the time at which the magnitude of the derivative decreases to below -5E-3 for at least 2 minutes is identified as steady state, i.e. after this time, very little additional varnish is removed with continued flow. Using this approach, we can determine that Fluid A's maximum varnish removal rate occurs, on average, 3.5 min after the test started and reached steady state at 17 min. For Fluid B, the maximum removal rate occurs at 12.2 min and reaches steady state at 48 min. This indicates that Fluid A reached its maximum removal rate and steady state removal sooner than Fluid B.

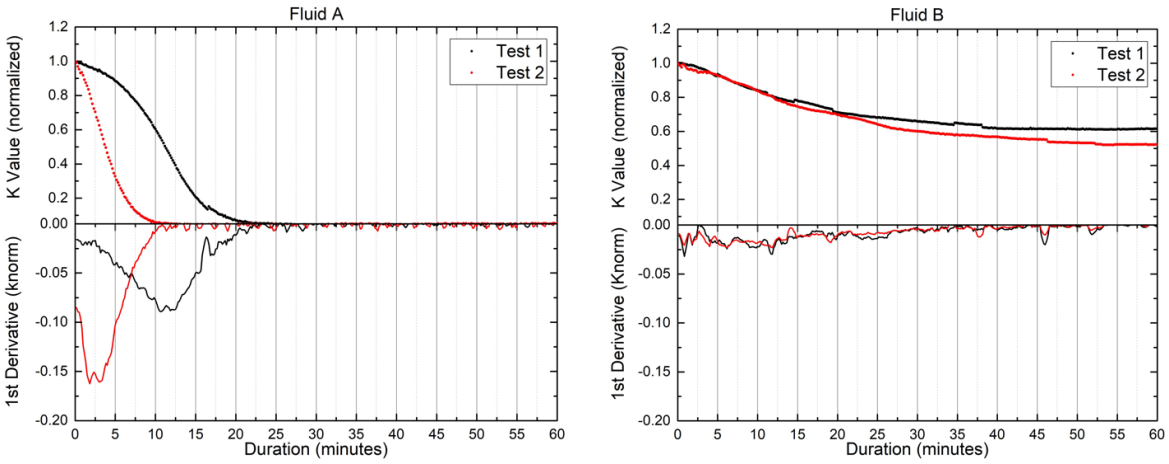

Figure 6: Time-lapse photographic results for Fluid A and Fluid B. Top portions of each graph display the normalized K value from the algorithm shown in Figure 5 while the bottom portions of the graphs show the 1st derivative of the normalized data. The derivative provides a means of identifying the time at which the varnish removal rate is a maximum and of steady state removal.

The analysis above enables quantitative comparison of times, but only qualitative comparison of the mass loss and rate of mass loss. To address this, the K values in Figure 6 need to be associated with mass removed. To determine the validity of this approach, the percent change of the normalized K value during the test is compared to the percent change of the coupon mass. The results are shown in Figure 7. The difference between the mass loss change and K value change is less than 4%, indicating that these two measures of total varnish removed are quite consistent. Based on this consistency, we can multiply the normalized K values by the start of test masses to general plots of varnish mass removed as a function of time.

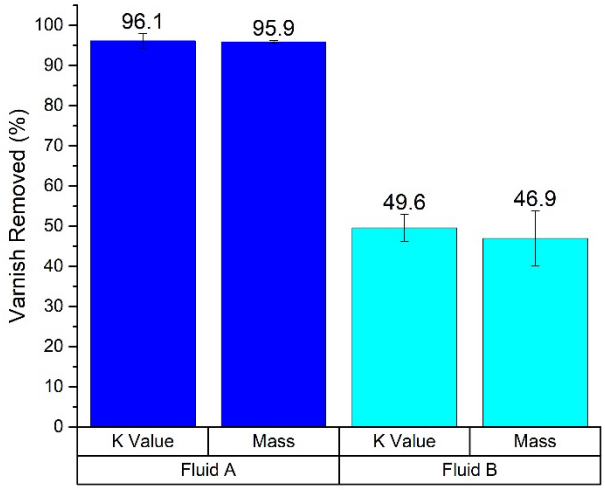

Figure 7: Percent varnish removed quantified by the total change in the normalized K factor during the test (green bars) and the difference between the coupon mass at the start and end of the test (cyan bars) for Fluids A and B.

Figure 8 shows the varnish removal in terms of mass as a function of time. Here, the data points at each time are calculated as an average from the two tests on each fluid. This result enables quantitative comparison of the fluids' varnish removal performance. We identify three parameters to fully characterize the varnish removal: maximum varnish removed, time at which the maximum varnish has been removed and maximum rate of varnish removal.

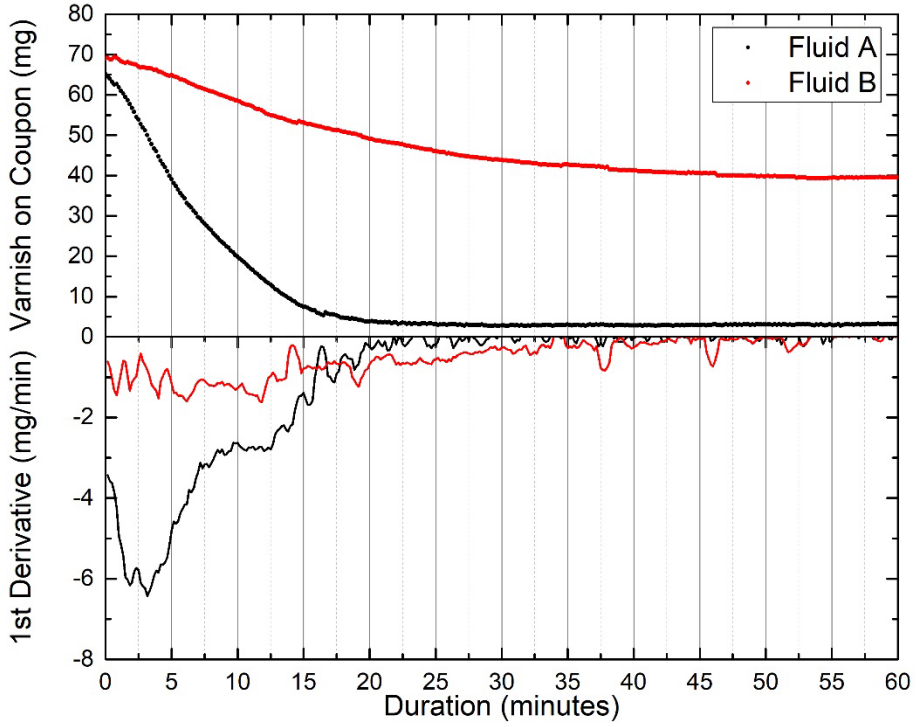

Figure 8: Top plot shows the average values for both fluids using the normalized K value multiplied by the original start of test varnish weight showing the actual weight of removal. The bottom plot shows the derivative of the varnish removal data.

Using the three characterization parameters mentioned above, a direct comparison between Fluid A and B can be made, as shown in Figure 9. In all cases, the parameters are averages from the two tests performed on each fluid. First, Fluid A removed substantially more varnish from the coupon than did Fluid B (95.9% vs 46.94%). The time required to reach steady state varnish removal is also shorter for Fluid A than Fluid B (17 min vs 48 min). Finally, Fluid A has a much larger maximum varnish removal rate than Fluid B (6.42 mg/min vs. 1.62 mg/min). Taken together, the comparison of these parameters shows that Fluid A is a much more aggressive chemical compound than Fluid B, removing twice as much varnish in half of the time.

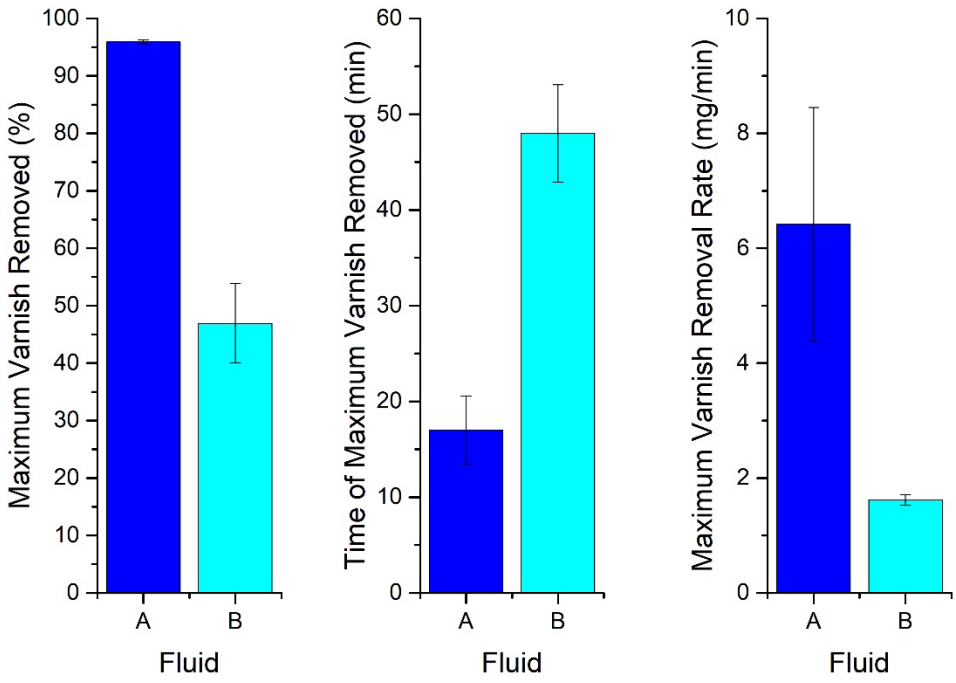

Figure 9: Comparison of Fluids A and B in terms of three varnish removal performance metrics. Left: maximum percent varnish removed. Center: time required to achieve steady state varnish removal. Right: maximum varnish removal rate.

CONCLUSION

Varnish is an unavoidable by-product of hydrocarbon oxidation that is exacerbated by heat, metals, entrained air, spark discharge and other factors. With the inevitable formation of varnish, methods of mitigating and removing varnish are critical to extending the life and performance of mechanical systems. Chemical flushes are a commonly used approach to varnish removal. However, there are a wide range of difference chemical compounds available for this purpose and, previously, there has not been a standard method of characterizing their effectiveness. To address this issue, we designed and constructed a test system capable of simulating the removal of varnish under realistic machine operating conditions. Two types of data are measured: the mass of varnish removed before and after the test and images of the coupon during testing. This data can be analyzed to yield three performance metrics: the percent varnish removed during the test, the time required to achieve steady-state varnish removal, and the maximum rate of varnish removal. The new approach is demonstrated here by applying it to compare two chemical flush compounds. The two fluids exhibit very different varnish removal performance, in which one removed varnish several times more quickly than the other, resulting in twice as much varnish removed in half the time. This example reveals the robustness of the test equipment design and of the post-test analyses. We anticipate that this test can provide a means of standardizing the removal of varnish using chemical flushes.

REFERENCES

1. Rudnick, L. R. (2009), “Lubricant Additives: Chemistry and Applications,” CRC press, Boca Raton, FL, ISBN 13:978-1-4200-5964-9.
2. Korcek, S., and Jensen, R. K. (1976), "Relation between base oil composition and oxidation stability at increased temperatures," ASLE Transactions, **19**(2), pp 83-94.
3. Fox M. F. (2010), “Chemistry and technology of lubricants,” 3rd Edition, Springer, London, NY, ISBN 978-1-4020-8661-8.
4. Sasaki, A. (2014) “Contaminants in Used Oils and Their Behavior,” Journal of ASTM International, **6**(2), pp 59-71.
5. Chen, L., Dong, J., and Chen, G. (1997), “The Study of Tribo-induced Deposits from a Copper-containing Antiwear Additive,” Tribology Transactions, **40**(2), pp 339-45.
6. Migdal, C. A., Wardlow, A. B., and Ameye, J. L., (2008), “Oxidation and the Testing of Turbine Oils,” ASTM International, West Conshohocken, PA.
7. Rounds F. (1993), “Effects of Hydroperoxides on Wear as Measured in Four-ball Wear Tests,” Tribology Transactions **36**(2), pp 297-303.
8. Atherton, B. (2007), “Discovering the root cause of varnish formation,” Practicing Oil Analysis, March 2, pp 22-5.
9. Kumar, N., Besuner, P., Lefton, S., Agan, D., Hilleman, D. (2012) “Power plant cycling costs,” National Renewable Energy Laboratory, Golden, CO.
10. Sitton, A., Ameye, J., Kauffman, R.E. (2006) “Residue Analysis on RPVOT Test Samples for Single and Multiple Antioxidants Chemistry for Turbine Lubricants,” Journal of ASTM International. **3**(6), pp 1-5.
11. Boyce, M.P. (2011), “Gas turbine engineering handbook.” Elsevier, Amsterdam, Netherlands.
12. Diaby, M., Sablier, M., Le Negrate, A., El Fassi, M., Bocquet, J. (2009) “Understanding carbonaceous deposit formation resulting from engine oil degradation,” Carbon **47**(2), pp 355-66.
13. Pirro, D.M., Webster, M., Daschner, E. (2016), “Lubrication Fundamentals, Revised and Expanded,” CRC Press, Boca Raton, FL.
14. Sasaki, A., Uchiyama, S., Yamamoto, T. (1999) “Free radicals and oil auto-oxidation due to spark discharges of static electricity” Tribology & Lubrication Technology **55**(9) pp 24.
15. Speight, J.G. (2014) “The chemistry and technology of petroleum,” CRC press, Boca Raton, FL.
16. Lantz, S., Zakarian, J., Deskin, S., Martini, A. (2017) “Filtration Effects on Foam Inhibitors and Optically Detected Oil Cleanliness,” Tribology Transactions **60**(6), pp 1-6.
17. ASTM D6439-11 (2017), “Standard Guide for Cleaning, Flushing, and Purification of Steam, Gas, and Hydroelectric Turbine Lubrication Systems”, ASTM International: West Conshohocken, PA.
18. ASTM D974-14e2 (2014), “Standard Test Method for Acid and Base Number by Color-Indicator Titration”, ASTM International: West Conshohocken, PA.
19. ASTM D664-17 (2017), “Standard Test Method for Acid Number of Petroleum Products by Potentiometric Titration,” ASTM International: West Conshohocken, PA.
20. ASTM D2272-14a (2014), “Standard Test Method for Oxidation Stability of Steam Turbine Oils by Rotating Pressure Vessel,” ASTM International: West Conshohocken, PA.
21. ASTM D445-17a (2017), “Standard Test Method for Kinematic Viscosity of Transparent and Opaque Liquids (and Calculation of Dynamic Viscosity),” ASTM International, West Conshohocken, PA.

22. ASTM D92-16b (2016), “Standard Test Method for Flash and Fire Points by Cleveland Open Cup Tester,” ASTM International: West Conshohocken, PA.
23. ASTM D7873-13 (2017), “Standard Test Method for Determination of Oxidation Stability and Insolubles Formation of Inhibited Turbine Oils at 120°C Without the Inclusion of Water (Dry TOST Method),” ASTM International: West Conshohocken, PA.